On the Reliability of Wireless Virtual Reality at Terahertz (THz) Frequencies

Christina Chaccour*, Ramy Amer[†], Bo Zhou*, and Walid Saad*

*Wireless@ VT, Bradly Department of Electrical and Computer Engineering, Virginia Tech, Blacksburg, VA USA,

†CONNECT, Trinity College, University of Dublin, Ireland.

Emails:{christinac, ecebo, walids}@vt.edu, ramyr@tcd.ie

Abstract—Guaranteeing ultra reliable low latency communications (URLLC) with high data rates for virtual reality (VR) services is a key challenge to enable a dual VR perception: visual and haptic. In this paper, a terahertz (THz) cellular network is considered to provide high-rate VR services, thus enabling a successful visual perception. For this network, guaranteeing URLLC with high rates requires overcoming the uncertainty stemming from the THz channel. To this end, the achievable reliability and latency of VR services over THz links are characterized. In particular, a novel expression for the probability distribution function of the transmission delay is derived as a function of the system parameters. Subsequently, the end-to-end (E2E) delay distribution that takes into account both processing and transmission delay is found and a tractable expression of the reliability of the system is derived as a function of the THz network parameters such as the molecular absorption loss and noise, the transmitted power, and the distance between the VR user and its respective small base station (SBS). Numerical results show the effects of various system parameters such as the bandwidth and the region of non-negligible interference on the reliability of the system. In particular, the results show that THz can deliver rates up to 16.4 Gbps and a reliability of 99.999%(with a delay threshold of 30 ms) provided that the impact of the molecular absorption on the THz links, which substantially limits the communication range of the SBS, is alleviated by densifying the network accordingly.

Index Terms—virtual reality (VR), terahertz, reliability, ultra reliable low latency communications (URLLC).

I. INTRODUCTION

Virtual reality (VR) is perhaps one of the most anticipated technologies of the coming decade [1]. However, relying on wired VR systems significantly limits the VR application domain. Instead, the deployment of wireless VR, over cellular networks, can potentially unleash its true potential [1], [2].

In order to integrate VR services over wireless networks, it is imperative to ensure ultra reliable low latency communications (URLLC) [2]. Predominantly, the end-to-end (E2E) delay for wireless VR needs very low (at the order of tens of milliseconds) in order to maintain a satisfactory user experience. Moreover, along with URLLC, wireless VR services will also require high data rates in order to deliver the 360° content to their users. Guaranteeing high data rates with URLLC requires a major departure from classical URLLC services that were limited to low-rate sensors [3]. To overcome this challenge, one can explore the high bandwidth available at the terahertz (THz) frequency bands which can enable high-rate wireless access for VR [4]. However, the reliability of the THz channel can be impeded by its susceptibility to blockage, molecular absorption, and communication range. Thus, it is imperative to understand whether THz frequencies can indeed provide an immersive VR experience by delivering URLLC at high rates.

A number of recent works attempted to address the challenges of VR communications [2], [5]–[8]. In [2], the authors discuss the current and future trends of wireless VR systems. The work in [5] introduces a perception-based mixed-reality video streaming delivery system to provide the aggregate data rates needed for VR services. In [6], the authors propose a VR model using multi-attribute utility theory to capture the tracking and delay components of VR quality-of-service (QoS). Meanwhile, the recent works in [7] and [8] study the problem of URLLC for VR networks. In [7], the issue of concurrent support of visual and haptic perceptions over wireless cellular networks is studied, while the work in [8] proposes a joint proactive computing and millimeter wave resource allocation scheme under latency and reliability constraints. However, these prior works [6]–[8] only examine the average delays and data rates; thus reflecting limited information about the systems analyzed. In contrast, to guarantee URLLC, it is necessary to have a full view of the statistics of the delay in order to properly characterize the system's reliability. Last, but not least, we note that the use of THz has recently attracted attention (e.g., see [9] and [4]) as an enabler of high data rate applications. However, these prior works in [9] and [4] do not address issues of reliability or low-latency for wireless VR systems. Clearly, there is a lack in existing works that study the potential of THz frequencies to deliver high-data rate VR services while providing URLLC.

The main contribution of this paper is to analyse the delay and reliability performance of a cellular network operating at THz frequencies and servicing VR users. The ultimate goal is to assess how and when a THz network can meet the dual requirements of the QoS of a VR user, in terms of URLLC and high data rates. In particular, we introduce a novel VR model based on a Matern hardcore point process (MHCPP). In the studied model, each VR user sends a request to its respective small base station (SBS), which induces an E2E delay that includes the delay needed to process the VR images and the transmission delay over the THz links. Based on this model, to find the cumulative distribution function (CDF) of the E2E delay, we derive the probability distribution function (PDF) of the transmission delay in a dense THz network. Subsequently, this allows us to derive the reliability of the system and to characterize the network parameters that affect this reliability. To our best knowledge, this is the first work that analyzes the reliability and latency achieved by VR services over a THz cellular network. Simulation results show that reliability is mainly affected by the transmission delay, which can be significantly reduced by providing the system with higher bandwidth or through densifying the network to maintain short-range communication between SBSs and users, thus overcoming the molecular absorption effects and guaranteeing reliability.

II. SYSTEM MODEL

Consider the downlink of a small cell network servicing a set $\mathcal V$ of V wireless VR users via a set of SBSs distributed in a confined indoor area according to an isotropic homogeneous MHCPP with intensity η and a minimum distance r [10]. This process is a special thinning of the Poisson point process (PPP) in which the nodes are forbidden to be closer than a minimum distance r. Here, the parameter r indicates that the distance between adjacent nodes cannot be arbitrarily small in the real-life phenomenon. Hence, this process can adequately capture the distribution of VR SBSs in a confined area. The SBSs can also perform mobile edge computing (MEC) functions for VR purposes.

A. Wireless Capacity

We consider an arbitrary VR user in V that is at a constant distance d_0 from its respective SBS. Hence, the chosen VR user and its respective SBS are referred to as tagged receiver and transmitter respectively. The interference surrounding this VR user stems from a set \mathcal{M} of M non-negligible interfering SBSs that are located within a radius of Ω around this user. This interference occurs because we consider a highly dense THz network whose SBSs are located at very close proximity. Henceforth, the SBSs that are at a distance $d > \Omega$ add no interference on the link between the VR user to its associated SBS. As shown in [11], the signal propagation at the THzband is mainly affected by molecular absorption, which results in molecular absorption loss and molecular absorption noise. Given that the distance between the VR user and its respective SBS is short in our model, we consider a line-of-sight (LoS) link only, as also done in [9]. Consequently, the total path loss affecting the transmitted signal between the SBS and the VR

user will be given by [11]:
$$L(f,d) = L_s(f,d)L_m(f,d) = \left(\frac{4\pi fd}{c}\right)^2 \frac{1}{\tau(f,d)}, \quad (1)$$

where $L_s(f,d)=(\frac{4\pi fd}{c})^2$ is the free-space propagation loss, $L_m(f,d)=\frac{1}{\tau(f,d)}$ is the molecular absorption loss, f is the operating frequency, d is the distance between the VR user and the SBS, c is the speed of light, and $\tau(f,d)$ is the transmittance of the medium following the Beer-Lambert law, i.e., $\tau(f,d)\approx \exp(-K(f)d)$, where K(f) is the overall absorption coefficient of the medium.

Let $d \triangleq (d_i)_{i=0,1,\cdots,M}$ be a row vector, where d_0 denotes the distance between the VR user and the associated SBS, and d_i denotes the distance between the VR user and the interfering SBS $i \in \mathcal{M}$. Let $p \triangleq (p_i)_{i=0,1,\cdots,M}$ be a row vector, where p_0 denotes the transmission power of the SBS servicing the considered VR user, and p_i denotes the transmission power of the interference from any other SBS $i \in \mathcal{M}$. The total noise power is the sum of the molecular absorption noise and the Johnson-Nyquist noise generated by thermal agitation of electrons in conductors. Consequently, the total noise power at the receiver can be given by [11]:

$$N(\mathbf{d}, p_i, f) = N_0 + \sum_{i=1}^{M} p_i A_o d_i^{-2} (1 - e^{-K(f)d_i}), \quad (2)$$

where $N_0=k_BT+p_{T_0}A_0d_0^{-2}(1-e^{-K(f)d_0})$, k_B is Botlzmann constant, T is the temperature in Kelvin, and $A_0=\frac{c^2}{16\pi^2f^2}$. Furthermore, accounting for the total path loss affecting the transmitted signal, the aggregate interference will be: $I(\boldsymbol{d},p_i,f)=\sum_{i=1}^M p_iA_od_i^{-2}e^{-K(f)d_i}$.

The instantaneous frequency-dependent signal-to-interference-plus-noise-ratio (SINR) is then given by:

$$S(\boldsymbol{d}, \boldsymbol{p}, f) = \frac{p_0^{\text{RX}}(d_0, p_0, f)}{I(\boldsymbol{d}, p_i, f) + N(\boldsymbol{d}, p_i, f)},$$
(3)

where $p_0^{\rm RX}$ is the received power at the VR user from its associated SBS. Substituting each of the received power, noise and interference term results in the following SINR:

$$S(\boldsymbol{d}, \boldsymbol{p}, f) = \frac{p_0 A_0 d_0^{-2} e^{-K(f)d_0}}{N_0 + \sum_{i=1}^{M} p_i A_o d_i^{-2}}.$$
 (4)

Hence, the capacity of the channel can be written as:

$$C(\boldsymbol{d}, \boldsymbol{p}, f) = W \log_2 \left(1 + \frac{p_0 A_0 d_0^{-2} e^{-K(f) d_0}}{N_0 + \sum_{i=1}^{M} p_i A_o d_i^{-2}} \right), \quad (5)$$

where W is the bandwidth.

B. Interference Analysis

From (5), we can see that the only random factor is the second term in the denominator which corresponds to the interfering signals. For technical tractability, following [11], we assume that this term tends to a normal distribution [12]. Note that, it has been shown in [11] that such an approximation is realistic. Furthermore, finding the mean and variance of this term will allow us to characterise the PDF of this random interference signal, as follows:

$$g(I) = \frac{1}{\sqrt{2\pi}\sigma_I} \exp\left(-\frac{(I - \mu_I)^2}{2\sigma_I^2}\right),\tag{6}$$

where μ_I and σ_I^2 are the mean and variance of the interference, respectively, and are given by [11]:

$$\mu_I = pA_0 \left(\frac{\ln(\Omega) - \ln(r)}{\Omega^2 - r^2} \right) \left(\frac{\pi \Omega^2 \eta}{2} \right), \tag{7}$$

$$\sigma_I^2 = (pA_0)^2 \left(\frac{\pi \Omega^2 \eta}{2}\right) \left(\frac{1}{2r^2 \Omega^2}\right),\tag{8}$$

where r is the minimum distance of the MHCPP, Ω is the region of non-negligible interference, and the subscript i in p_i is omitted given that the SBSs are assumed to have the same transmission power. As shown in [11], μ_I and σ_I can be derived based upon the Poisson approximation for the distances between the tagged receiver and the interferers. Given the high bandwidth available at the THz band can provide high-rate wireless VR, however, it is necessary to analyze whether this network can provide URLLC. Next, we will analyze the delay of the considered system and, then, leverage this analysis to define reliability.

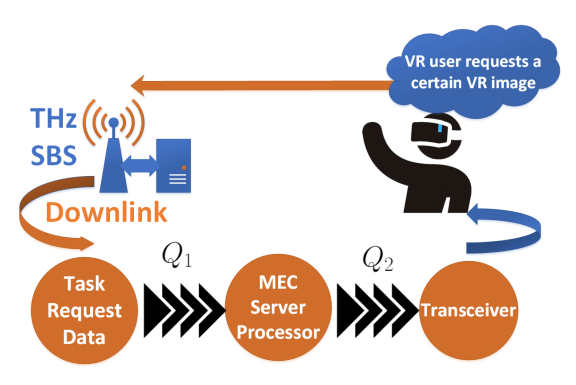


Figure 1: Illustrative example of our system model.

III. RELIABILITY ANALYSIS

A. Delay Analysis

The service model of the VR image request in our wireless VR system is illustrated in Fig. 1. As shown, once a VR user requests a VR image, this request will go through two queues: a first queue, Q_1 , that pertains to processing a 360° VR image, and a second queue, Q_2 , that pertains to storing and transmitting the VR images over the wireless THz channel. Here, we assume that the time for sending a request by the VR user is negligible. Hence, for each VR image request, the total delay depends on the waiting and the processing time at Q_1 and the waiting time and VR transmission delay at Q_2 .

We assume that a VR image request follows a Poisson arrival process with mean rate λ_1 . The buffer of the processor is assumed to be of infinite size and the MEC processor at the SBS adopts the first-come, first-serve (FCFS) policy. The service time for each request follows an exponential distribution with rate parameter $\mu_1 > \lambda_1$, to guarantee the stability of the first queue Q_1 . Thus, we can see that the queue Q_1 is an M/M/1 queue. According to Burke's theorem [13], when the service rate is larger than the arrival rate for an M/M/1 queue, then the departure process at steady state is a Poisson process with the same arrival rate. Hence, the arrival of requests to Q_2 also follows a Poisson process with rate $\lambda_2 = \mu_1$. Similar to Q_1 , we assume an infinite buffer size and an FCFS policy for Q_2 . Note that, the service time of Q_2 is the transmission time of the SBS, that depends on the random wireless THz channels. Thus, different from Q_1 , the second queue Q_2 is an M/G/1 queue.

Our goal is to study when and how the proposed THz system can guarantee the dual QoS requirement required by VR, i.e. visual and haptic perceptions. This dual perception requires a high data rate link for visual perception and a low latency communication for the haptic. Under favorable channel conditions, THz is capable of providing high rate links, however, providing URLLC may be challenging. Hence, our key step is to define the reliability of this system and study the performance of the VR network. This performance analysis will shed light on the capability of THz to provide a dual-metric performance for VR. To analyze reliability, next, we first derive the PDF of the transmission delay of our THz network. This expression will then be used to derive the CDF of the E2E delay characterizing the reliability of the system

and the QoS. It is important to note that reliability cannot be defined merely on average values of delays as done in [6] and [2]. Given the stringent requirements of VR services, a full view on the statistics of the delay must be to be taken into account in order to design a system capable of withstanding extreme and infrequently occurring events such as a sudden user movement that changes its distance from its respective SBS or a sudden blockage between the user and the SBS which can impact reliability.

B. Reliability Analysis

The reliability of the considered wireless VR system can be defined as a guarantee that the E2E delay can be maintained below a target threshold δ . Formally, reliability is the probability that the E2E delay – defined as the delay incurred between the time the VR user requests a VR image to the time the image is received – remains below δ . Hence, the system is guaranteed to have high reliability when this probability is high and tends to 1.

For our model in Fig. 1, given that Q_1 is an M/M/1 queue, the PDF of the total waiting time at Q_1 will be [13]:

$$\psi_1(t) = (\mu_1 - \lambda_1) \exp(-(\mu_1 - \lambda_1)t). \tag{9}$$

Moreover, given that Q_2 is an M/G/1 queue and that the queuing and service time of an M/G/1 queue are independent, we can derive that the CDF of the total waiting time:

$$\Psi_2(t) = \Psi_{O_2}(t) * \psi_T(t), \tag{10}$$

where * is the convolution operator, $\Psi_{Q_2}(t)$ is the CDF of the queuing time at Q_2 and $\psi_T(t)$ is the PDF of the transmission delay. The CDF of the total queuing time at Q_2 will be [13]:

delay. The CDF of the total queuing time at
$$Q_2$$
 will be [13]:
$$\Psi_{Q_2(t)} = (1 - \rho) \sum_{n=0}^{\infty} \left[\rho^n R^{(n)}(t) \right], \tag{11}$$
 where $\rho = \frac{\lambda_2}{\mu_2}$ is the utilization factor, λ_2 and μ_2 are the arrival

where $\rho=\frac{\lambda_2}{\mu_2}$ is the utilization factor, λ_2 and μ_2 are the arrival and average transmission rates of Q_2 , respectively. Here, Γ is the number of states that the queue has went through, i.e., the number of packets that has passed through the queue during a certain amount of time and $R^{(n)}(t)$ is the CDF of the residual service time after the n-th state. Note that $R^{(n)}(t)$ can be computed by obtaining the residual service time distribution R(t) after n packets, $R(t)=\int_0^t \mu_2(1-\psi_T(x))dx$, where t is the time of an arbitrary arrival, given that the arrival occurs when the server is busy. To evaluate the PDF of the E2E delay, we need the PDF of the transmission delay which is found next:

Lemma 1. The PDF of the transmission delay is given by:

$$\psi_T(\alpha) = \frac{\zeta}{\sqrt{2\pi}\sigma_I} \exp\left(\frac{(\Upsilon - \mu_I)^2}{2\sigma_I^2}\right),\tag{12}$$

where

$$\zeta = \frac{\ln(2)(p_0^{RX}L)2^{\frac{L}{W\alpha}}}{W\alpha^2(2^{\frac{L}{W\alpha}}-1)^2},$$
(13)

$$\Upsilon = \frac{(1 - 2\frac{L}{W\alpha})N_0 + p_0^{RX}}{2\frac{L}{W\alpha} - 1},\tag{14}$$

where L is the packet size and α is the transmission delay.

Proof: Based on (5), we express the capacity in terms of L and α as:

$$C = \frac{L}{\alpha} = W \log_2 \left(1 + \frac{p_0 A_0 d_0^{-2} e^{-K(f) d_0}}{N_0 + \sum_{i=1}^M p A_o d_i^{-2}} \right), \tag{15}$$

We can see that the only random term in (15) is the interference that is assumed to follow a normal distribution. Subsequently, we can express the interference in terms of the transmission delay α as follows:

$$\sum_{i=1}^{M} p A_o d_i^{-2} = \frac{N_0 \left(1 - 2 \frac{L}{W\alpha} \right) + p_0^{\text{RX}}}{2 \frac{L}{W\alpha} - 1}.$$
 (16)

By applying the transform for PDFs $g(y)=g(x)\frac{\partial x}{\partial y}$ we can find the PDF of transmission delay by transforming the PDF of interference accordingly. We let Υ represent the interference and ζ its derivative with respect to the transmission delay. Then we have:

Then, we have:
$$\Upsilon = \sum_{i=1}^{M} p_i A_o d_i^{-2}, \tag{17}$$

$$\zeta = \frac{d\Upsilon}{d\alpha} = \frac{\ln(2) \ln \cdot 2^{\frac{L}{W\alpha}}}{W\alpha^2 \left(2^{\frac{L}{W\alpha}} - 1\right)} + \frac{\ln(2) L\left(N_0 \left(1 - 2^{\frac{L}{W\alpha}}\right) + p_0^{\text{RX}}\right) \cdot 2^{\frac{L}{W\alpha}}}{W\alpha^2 \left(2^{\frac{L}{W\alpha}} - 1\right)^2} = \frac{\ln(2) L p_0^{\text{RX}} \cdot 2^{\frac{L}{W\alpha}}}{W\alpha^2 \left(2^{\frac{L}{W\alpha}} - 1\right)^2}. \tag{18}$$

Hence, the transmission delay PDF will be:

$$\psi_T(\alpha) = g(\Upsilon) \frac{d\Upsilon}{d\alpha} = \zeta g(\Upsilon)$$

$$= \frac{\zeta}{\sqrt{2\pi}\sigma_I} \exp\left(\frac{(\Upsilon - \mu_I)^2}{2\sigma_I^2}\right). \tag{19}$$

It is important to note that the PDF in (19) does not follow a normal distribution since both Υ and ζ depend on the transmission delay α . Burke's Theorem allows us to infer that Q_1 and Q_2 are independent; therefore, the CDF of the E2E delay can be expressed as the convolution of the PDF of the total waiting time in Q_1 and the CDF of the total waiting time in Q_2 . By using the dynamics of (9) and (10), the CDF of the E2E delay can formally expressed in the following theorem which is a direct result of Lemma 1.

Theorem 1. The CDF of the E2E delay T_e is given by:

$$\Phi(t) = P(T_e \le t) = \psi_1(t) * \Psi_2(t)$$

$$= \psi_1(t) * (\Psi_{Q_2}(t) * \psi_T(t))$$

$$= (\mu_1 - \lambda_1) \exp(-(\mu_1 - \lambda_1)t)$$

$$* \left((1 - \rho) \sum_{n=0}^{\Gamma} (\rho^{\Gamma} R^{(n)}(t)) \right)$$

$$* \left(\frac{\zeta}{\sqrt{2\pi}\sigma_I} \exp\left(\frac{(\Upsilon - \mu_I)^2}{2\sigma_I^2}\right) \right). \quad (20)$$

Consequently, the *reliability* can be defined as the probability of the E2E delay not exceeding a certain threshold δ , i.e.,

$$\varrho = P(T_e \le \delta) = \Phi(\delta). \tag{21}$$

The reliability in (21) allows a tractable characterization of the reliability of the VR system shown in Fig. 1, as function of the THz channel parameters. Furthermore, from Theorem 1, we can first see that the queuing time of Q_2 depends on the residual service time CDF and hence on the transmission delay. Also, given that the processing speed of the MEC servers can be considerably high, the E2E delay will often be dominated by the transmission delay of THz. Moreover, in general, all the key parameters that have a high impact on the transmission delay will have a higher impact on reliability. One of the most important key parameters is the distance d_0 between the VR user and its respective SBS; this follows from the fact that the molecular absorption loss gets significantly higher when the distance increases, which limits the communication range of THz SBSs to very few meters. Indeed, the THz reliability will deteriorate drastically if the distance between the VR user and its respective SBS increased.

Given that the QoS of a VR application is a function of the reliability, i.e., it is the reliability of the system throughout the worst case scenario. VR users' immersion and experience will depend significantly on the reliability. Therefore, maintaining reliability is a necessary condition to guarantee the QoS for the user, thus increasing its satisfaction and yielding it a seamless experience.

IV. NUMERICAL RESULTS

For our simulations, we consider the following parameters: $T=300\,\mathrm{K},\ p=1\,\mathrm{W},\ L=10\,\mathrm{Mbits},\ f=1\,\mathrm{THz},\ K(f)=0.0016\,\mathrm{m}^{-1}$ with 1% of water vapor molecules as in [14], $\lambda_1=0.1\,\mathrm{packets/s},$ and $\mu_1=2\,\mathrm{Gbps}.$ These values are chosen to comply with existing VR processing units such as the GEFORCE RTX 2080 Ti [15]. The SBSs are deployed in an indoor area modeled as a square of size $20\,\mathrm{m}\times20\,\mathrm{m}.$ All statistical results are averaged over a large number of independent runs.

Fig. 2 shows that the simulation results match the distribution of the analytical result derived in (12). The small gap between the analytical and simulation results stems from the normal distribution of the interference.

Fig. 3 (a) shows the prominent effect of the bandwidth on the reliability at different δ . We can see that the reliability monotonically increases with both the bandwidth and reliability threshold δ . Subsequently, we can see that, in order to achieve a reliability of 99.999% at δ =30ms, we need a bandwidth of 10 GHz. For our THz system, this corresponds to a data rate of 16.4 Gbps. Clearly, the target reliability for VR services can be achieved with high rates at THz frequencies, assuming sufficient bandwidth is available. Furthermore, the reliability for δ = 10 ms saturates around W = 12 GHz. This is due to the fact that the delay in Q_2 has reached a point where it is equal to the delay in Q_1 in Fig.3(b); after that point, the delay becomes dominated by the delay in Q_1

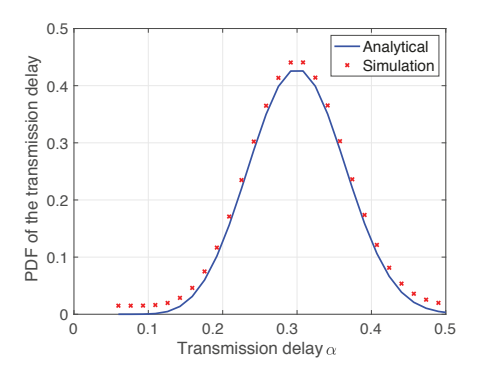


Figure 2: PDF of the transmission delay.

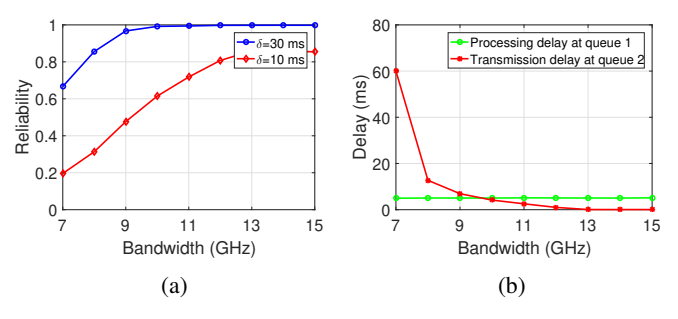


Figure 3: Effect of bandwidth on the achievable performance (a) Reliability versus bandwidth, (b) Delay versus bandwidth.

rather than Q_2 . Furthermore, a very high reliability cannot be achieved for $\delta=10\,\mathrm{ms}$ in Fig. 3 (a) due to the delay at Q_1 . Hence, the limitation in reliability for a very low threshold, namely $\delta=10\,\mathrm{ms}$ is mainly a result of the processing speed at the MEC server. Also, it is important to note that before the point of saturation, the reliability is mainly dominated by the transmission delay which confirms the result obtained in (20).

In Fig. 4, we show how the reliability varies as a function of the region of non-negligible interference. We can see that, when the distance between the VR user and the SBS increases, the region of non-negligible interference Ω has a higher impact on the reliability, and the drop of reliability is sharper. This phenomenon is observed regardless of the reliability threshold δ . Hence, even though the user can achieve high reliability, the dependence of the molecular absorption on distance limits the user to a very short distance to its respective SBS. Thus, the VR user can guarantee reliability regardless of the interference surrounding it, given that it is at a proximity from the respective SBS.

V. CONCLUSION

In this paper, we have studied the reliability of VR services deployed in a THz cellular network. To obtain an expression for the end-to-end delay and reliability, we have proposed a model based on a two tandem queue. We have derived the PDF of the transmission delay of a THz cellular network, based on which, we have derived the E2E delay expression along with the reliability of this system. We have shown that operating at THz frequencies can potentially enable VR services to have high reliability and high rates when provided with high

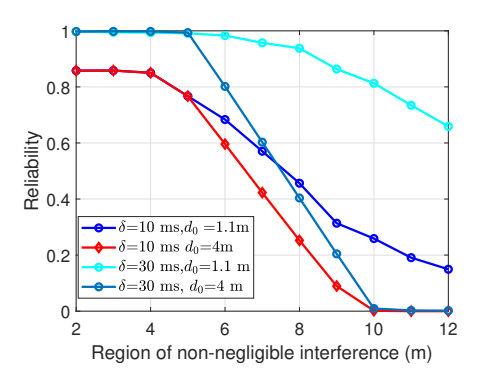


Figure 4: Reliability versus region of non-negligible interference.

bandwidth and proximity to the respective SBS. Hence, the design of these networks requires managing a tradeoff between the bandwidth used and the average proximity of the user to the respective SBS.

REFERENCES

- W. Saad, M. Bennis, and M. Chen, "A vision of 6G wireless systems: Applications, trends, technologies, and open research problems," arXiv preprint arXiv:1902.10265, 2019.
- [2] M.Bamby, C. Perfecto, M. Bennis, and K. Doppler, "Towards low-latency and ultra-reliable virtual reality," *IEEE Network*, vol. 32, no. 2, pp. 78–84, Apr. 2018.
- [3] G. Gerardino, B. Alvarez, K. Pedersen, and P. Mogensen, "MAC layer enhancements for ultra-reliable low-latency communications in cellular networks," in *Proc. IEEE International Conference on Communications* (ICC), Paris, France, pp. 1–7.
- [4] A. Moldovan, P. Karunakaran, I. F. Akyildiz, and W. H. Gerstacker, "Coverage and achievable rate analysis for indoor terahertz wireless networks," in *Proc. IEEE International Conference on Communications* (ICC), Paris, France, Jul. 2017, pp. 1–7.
- [5] K. Doppler, E. Torkildson, and J.Bouwen, "On wireless networks for the era of mixed reality," in *Proc. European Conference on Networks* and Communications (EuCNC), Oulu, Finland, Jun. 2017.
- [6] M.Chen, W. Saad, and C. Yin, "Virtual reality over wireless networks: Quality-of-service model and learning-based resource management," *IEEE Transactions on Communications*, vol. 66, no. 11, pp. 5621–5635, Jun. 2018.
- [7] J. Park and M. Bennis, "URLLC-eMBB slicing to support VR multi-modal perceptions over wireless cellular systems," in *Proc. IEEE Global Communications Conference (GLOBECOM)*, Abu Dhabi, UAE, Dec. 2018.
- [8] M.S.Elbamby, C. Perfecto, and M. Bennisand K. Doppler, "Edge computing meets millimeter-wave enabled VR: Paving the way to cutting the cord," in *Proc. IEEE Wireless Communications and Networking Conference (WCNC)*, Barcelona, Spain, Apr. 2018.
- [9] A. S. Cacciapuoti, R. Subramanian, K. R. Chowdhury, and M. Caleffi, "Software-defined network controlled switching between millimeter wave and terahertz small cells," arXiv preprint arXiv:1702.02775, 2017.
- [10] M. Haenggi, Stochastic geometry for wireless networks. Cambridge University Press, 2012.
- [11] V. Petrov, D. Moltchanov, and Y. Koucheryavy, "Interference and SINR in dense terahertz networks," in *Proc. IEEE 82nd Vehicular Technology Conference (VTC2015-Fall)*, Boston, MA, USA, Sep. 2015, pp. 1–5.
- [12] A. V. Pechinkin, "On convergence of random sums of random variables to the normal law," *Teoriya Veroyatnostei i ee Primeneniya*, vol. 18, no. 2, pp. 380–382, 1973.
- [13] D. Gross, J. F. Shortle, J. Thompson, and C. M.Harris, Fundamentals of Queuing Theory. Hoboken, New Jersey, USA: John Wiley Sons, Inc., 1974.
- [14] C.-C. Wang, X.-W. Yao, C. Han, and W.-L. Wang, "Interference and coverage analysis for terahertz band communication in nanonetworks," in *Proc. IEEE Global Communications Conference (GLOBECOM)*, Singapore, Singapore, Jan. 2018.
- [15] GEFORCE® RTX 2080 Ti. [Online]. Available: https://www.nvidia.com/en-us/geforce/graphics-cards/rtx-2080-ti/